Eur. Phys. J. C (2018) 78:574
https://doi.org/10.1140/epjc/s10052-018-6045-0

THE EUROPEAN PHYSICAL JOURNAL C

Regular Article - Theoretical Physics

Khuri–Treiman equations for $\pi\pi$ scattering

M. Albaladejo[1,a], N. Sherrill[2,3,b], C. Fernández-Ramírez[4], A. Jackura[2,3], V. Mathieu[5], M. Mikhasenko[6], J. Nys[2,3,5,7], A. Pilloni[5], A. P. Szczepaniak[2,3,5], Joint Physics Analysis Center

[1] Departamento de Física, Universidad de Murcia, 30071 Murcia, Spain
[2] Center for Exploration of Energy and Matter, Indiana University, Bloomington, IN 47403, USA
[3] Physics Department, Indiana University, Bloomington, IN 47405, USA
[4] Instituto de Ciencias Nucleares, Universidad Nacional Autónoma de México, 04510 Mexico City, Mexico
[5] Theory Center, Thomas Jefferson National Accelerator Facility, Newport News, VA 23606, USA
[6] Helmholtz-Institut für Strahlen- und Kernphysik, Universität Bonn, 53115 Bonn, Germany
[7] Department of Physics and Astronomy, Universiteit Gent, Gent, Belgium

Received: 28 March 2018 / Accepted: 2 July 2018 / Published online: 13 July 2018

Abstract The Khuri–Treiman formalism models the partial-wave expansion of a scattering amplitude as a sum of three individual truncated series, capturing the low-energy dynamics of the direct and cross channels. We cast this formalism into dispersive equations to study $\pi\pi$ scattering, and compare their expressions and numerical output to the Roy and GKPY equations. We prove that the Khuri–Treiman equations and Roy equations coincide when both are truncated to include only S- and P-waves. When higher partial waves are included, we find an excellent agreement between the Khuri–Treiman and the GKPY results. This lends credence to the notion that the Khuri–Treiman formalism is a reliable low-energy tool for studying hadronic reaction amplitudes.

1 Introduction

Three-body decays offer a unique window into hadron dynamics. They are an especially useful tool for exploring the hadron spectrum in the *exotic* sectors, where resonances appear that cannot be accurately described by constituent quark models. Some notable examples are the mysterious XYZ peaks observed in three-body decays of heavy quarkonia [1–3]. Moreover, new methods have recently been developed that enable direct mapping from three-particle spectra in a finite volume to three-particle scattering amplitudes in the infinite volume, opening the door to lattice QCD calculations [4–6]. Generally speaking, robust methods for constructing reaction amplitudes that fulfill well-known properties from S-matrix theory, such as analyticity, unitarity, and crossing symmetry for the analysis of three-particle final states are mandatory.

One of the main issues posed by the presence of hadrons in any reaction is their final-state interactions, which are formally expressed in terms of the unitarity of the T-matrix. In the case of $2 \to 2$ scattering, this effect can often be incorporated by neglecting unitarity in the t- and u-channels while preserving s-channel unitarity. For example, in the case of $\pi\pi$ scattering, the results obtained for the σ meson with the Roy equations (or other dispersive approaches that account for the left-hand cut singularities in a nonperturbative way) are very similar to those obtained with approaches that neglect altogether the left-hand cut, or take it into account perturbatively (see for example Refs. [7–9] and references therein). Despite crossing symmetry, this is certainly not the case for a $1 \to 3$ decay, where ideally one wants to take into account unitarity in the three possible two-hadron channels in the final state.

In the 1960s, Khuri and Treiman proposed a simple amplitude model to study $K \to 3\pi$ decays [10]. This model is based on the factorization of the scattering amplitude $A(s,t,u)$ into a sum of three functions, each of which depends on a single Mandelstam variable only. Several more studies later appeared that expanded upon this representation of the amplitude [11–16] (see also the recent lectures in Ref. [17]). For the lowest waves, this approach, which we refer to as the Khuri–Treiman (KT) formalism, can be justified in chiral perturbation theory (χPT) at lowest order via the so-called reconstruction theorem [18–20]. From a broader point of view, as we will discuss in detail below, the KT formalism is a rather simple approach for modeling $A(s,t,u)$. Generally speaking, an infinite sum of s-channel partial waves that contain both right-hand cut (RHC) and left-hand cut (LHC)

[a] e-mail: miguelalbaladejo@gmail.com
[b] e-mail: nlsherri@iu.edu

discontinuities is substituted by a finite sum of s-, t-, and u-channel *isobar* amplitudes, each of which exhibit only a RHC structure emanating from unitarity in the respective channel. Although it is known that this model fails to properly account for asymptotic behavior at high energies, it is expected to accurately describe the physics at low energies. For this reason, it has often been used to study meson decays, where the energy range is limited by the decay kinematics. This formalism has recently been reviewed and applied to various three-body decay channels of light and heavy mesons [21–32].

Because the KT formalism has been applied to such a wide range of processes, it is important to establish and validate its range of applicability. This is what we propose to do in this paper. Specifically, we compare the KT model amplitude for $\pi\pi$ scattering with the results of other, arguably more sophisticated dispersive approaches. In the same spirit, we will not strictly enforce elastic unitarity, unlike in Refs. [10,21–32]. The manuscript is organized as follows. In Sect. 2 we present our notation for the general description of $\pi\pi$ scattering, as well as the form of the scattering amplitude in the KT formalism. In Sect. 3 we analytically compare the KT and Roy equations [33] for the lowest partial waves. We explicitly demonstrate that both formalisms exactly coincide when truncated to S- and P-waves, complementing former results discussed in Refs. [34–39]. In Sect. 4 we numerically study the results obtained with the KT equations considering also D- and F-waves, using as an input the parameterization of the $\pi\pi$ scattering shift in Ref. [40]. We compare the results obtained with the latter parameterization and with the results of the GKPY equations discussed in the same work. The conclusions are given in Sect. 5. In the Appendix we specifically discuss the contributions of the LHC to the partial waves.

2 Amplitudes

We begin by briefly reviewing the structure of $\pi\pi$ scattering as it relates to our analysis of the KT equations. The general form of the isopin invariant $\pi\pi$ scattering amplitude is determined from the matrix elements of the transition-matrix operator $\hat{T}$:

$$\begin{aligned}\frac{1}{32\pi}\langle\pi_k(p_3)\pi_l(p_4)|\hat{T}|\pi_i(p_1)\pi_j(p_2)\rangle &\equiv A_{ijkl}(s,t,u)\\ &= \delta_{ij}\delta_{kl}A(s,t,u)+\delta_{ik}\delta_{jl}A(t,s,u)+\delta_{il}\delta_{jk}A(u,t,s).\end{aligned} \tag{1}$$

The Latin indices in Eq. (1) denote Cartesian isospin indices.[1] The variables s, t, and u refer to the usual Mandelstam variables. In addition, the invariant amplitude can be expressed in terms of a single function $A(s,t,u)$ and permutations of its arguments by virtue of crossing symmetry. Bose symmetry also requires this function to be symmetric in the second and third variable, $A(s,t,u) = A(s,u,t)$. Our primary interest in the structure $A_{ijkl}(s,t,u)$ is its decomposition into amplitudes of well-defined isospin in the s-channel, $A^{(I)}(s,t,u)$, which is accomplished by means of projectors:

$$A_{ijkl}(s,t,u) = \sum_{I=0}^{2} P^{(I)}_{ijkl}\, A^{(I)}(s,t,u), \tag{2}$$

$$\begin{aligned}P^{(0)}_{ijkl} &= \frac{1}{3}\delta_{ij}\delta_{kl},\\ P^{(1)}_{ijkl} &= \frac{1}{2}\left(\delta_{ik}\delta_{jl}-\delta_{il}\delta_{jk}\right),\\ P^{(2)}_{ijkl} &= \frac{1}{2}\left(\delta_{ik}\delta_{jl}+\delta_{il}\delta_{jk}\right)-\frac{1}{3}\delta_{ij}\delta_{kl}.\end{aligned} \tag{3}$$

The amplitudes $A^{(I)}(s,t,u)$ can be written, in turn, as combinations of the amplitude $A(s,t,u)$ and permutations of the arguments by comparing Eqs. (1) and (2):

$$\begin{aligned}\begin{bmatrix}A^{(0)}(s,t,u)\\ A^{(1)}(s,t,u)\\ A^{(2)}(s,t,u)\end{bmatrix} &= \begin{bmatrix}3 & 1 & 1\\ 0 & 1 & -1\\ 0 & 1 & 1\end{bmatrix}\begin{bmatrix}A(s,t,u)\\ A(t,s,u)\\ A(u,t,s)\end{bmatrix}\\ &\equiv K\begin{bmatrix}A(s,t,u)\\ A(t,s,u)\\ A(u,t,s)\end{bmatrix}.\end{aligned} \tag{4}$$

The left-hand side of Eq. (4) can be decomposed into an infinite series of s-channel partial-wave amplitudes $t_l^{(I)}(s)$:

$$A^{(I)}(s,t,u) = \sum_{\ell=0}^{\infty}(2\ell+1)P_\ell(z_s)t_\ell^{(I)}(s), \tag{5}$$

$$t_\ell^{(I)}(s) = \frac{1}{2}\int_{-1}^{+1}\mathrm{d}z_s\, P_\ell(z_s)A^{(I)}(s,t(s,z_s),u(s,z_s)), \tag{6}$$

where $P_\ell(z_s)$ are Legendre polynomials in the variable z_s, the s-channel scattering angle, which has the form

$$z_s = z_s(s,t,u) = \frac{t-u}{4p^2(s)}. \tag{7}$$

Additionally, the cross-channel variables under this projection are given by

$$t(s,z_s) = -2p^2(s)(1-z_s), \tag{8}$$

$$u(s,z_s) = -2p^2(s)(1+z_s), \tag{9}$$

where $p^2(s) = (s-4m^2)/4$ is the momentum squared in the center-of-mass frame, and m is the charge-averaged pion mass. The normalization of the partial-wave amplitudes is chosen such that

$$t_\ell^{(I)}(s) = \frac{\eta_\ell^{(I)}(s)e^{2i\delta_\ell^{(I)}(s)}-1}{2i\sigma(s)}, \tag{10}$$

[1] For a detailed derivation of this decomposition we refer the reader to Refs. [41,42].

where $\sigma(s) = \sqrt{1-\frac{4m^2}{s}} = 2p(s)/\sqrt{s}$. The threshold parameters (which are dimensionless with our definitions) are defined through

$$\frac{m^{2\ell}}{p^{2\ell}(s)}\mathrm{Re}\, t_\ell^{(I)}(s) = a_\ell^{(I)} + b_\ell^{(I)}\frac{p^2(s)}{m^2} + \cdots . \tag{11}$$

We now wish to describe the amplitude $A(s,t,u)$ within the KT formalism. This involves truncating the infinite series of s-channel partial-wave amplitudes $t_\ell^{(I)}(s)$, which contain both RHC and LHC structure. Truncating this expansion at some maximum orbital angular momentum $\ell_{\max}$ defines an amplitude that is regular in the variables t and u. The singularities generated by t- and u-channel physics can be partially recovered by adding truncated t- and u-channel series expansions of partial-wave-like functions [24,28,31,43]:

$$\begin{aligned} A(s,t,u) = &\sum_{\ell=0}^{\ell_{\max}}(2\ell+1)P_\ell(z_s)p^{2\ell}(s)a_\ell^s(s) \\ &+(s\to t)+(s\to u)\,, \end{aligned} \tag{12}$$

where the functions $a_\ell^s(s)$, $a_\ell^t(t)$, and $a_\ell^u(u)$ are isobars in the indicated channel. By assumption, the isobars contain only RHC singularities in their respective channel variable and thus exclusively account for the singularity structure of $A(s,t,u)$. It is important to recognize that the isobars are not independent functions: the symmetry $A(s,t,u) = A(s,u,t)$ implies $a_\ell^t(t) = (-1)^\ell a_\ell^u(t)$. Note that crossing symmetry is respected in Eq. (12) since we take $\ell_{\max}$ to be the same integer for each truncated series and the inclusion of the $p^{2\ell}$ factors enforces the proper behavior of $A(s,t,u)$ near threshold [44,45]. As we mentioned in the introduction, this representation of the amplitude is consistent with the reconstruction theorem [18], but only if $\ell_{\max} \leqslant 1$. In this regard, the representation given by Eq. (12) is more general, however, its effectiveness is restricted to low energies and partial waves, as it lacks Mandelstam analyticity in the angular momentum plane. We accept the limitations of this representation and aim to test the limits of its effectiveness.

From here, we construct isobars of definite isospin in the s-channel and denote them as $\bar{a}_\ell^{(I)}(s)$. These can be defined by comparing the KT amplitude in Eq. (12) with Eq. (4). Specifically, we define:

$$\begin{bmatrix} \bar{a}_\ell^{(0)}(x) \\ \bar{a}_\ell^{(1)}(x) \\ \bar{a}_\ell^{(2)}(x) \end{bmatrix} = K \begin{bmatrix} a_\ell^s(x) \\ a_\ell^t(x) \\ a_\ell^u(x) \end{bmatrix}, \tag{13}$$

where $x = s,t,u$ and the matrix K has been introduced in Eq. (4). Using this relation in Eq. (12) we obtain

$$\begin{aligned} A(s,t,u) = &\sum_{\ell=0}^{\ell_{\max}}(2\ell+1)P_\ell(z_s)p^{2\ell}(s)\frac{\bar{a}_\ell^{(0)}(s)-\bar{a}_\ell^{(2)}(s)}{3} \\ &+\sum_{\ell=0}^{\ell_{\max}}(2\ell+1)P_\ell(z_t)p^{2\ell}(t)\frac{\bar{a}_\ell^{(1)}(t)+\bar{a}_\ell^{(2)}(t)}{2} \\ &+\sum_{\ell=0}^{\ell_{\max}}(2\ell+1)P_\ell(z_u)p^{2\ell}(u)\frac{\bar{a}_\ell^{(1)}(u)+\bar{a}_\ell^{(2)}(u)}{2}(-1)^\ell, \end{aligned} \tag{14}$$

where z_t and z_u are the t- and u-channel center-of-mass scattering angles,

$$z_t = z_t(s,t,u) = \frac{s-u}{4p^2(t)}, \tag{15}$$

$$z_u = z_u(s,t,u) = \frac{t-s}{4p^2(u)}. \tag{16}$$

For the rest of the paper we will use the condensed notation $z_t(s,z) = z_t(s,t(s,z),u(s,z))$ and the analogous notation for z_u. In Eq. (14) it should be understood that $\bar{a}_\ell^{(I)} = 0$ unless $\ell + I$ is an even integer so that Bose symmetry is respected. We remind the reader that the specific choice of the nomenclature in Eq. (14) is such that the well-defined isospin amplitudes $A^{(I)}(s,t,u)$ have isobars $\bar{a}_\ell^{(I)}(s)$ in the s-channel projection. More specifically, inserting Eq. (14) into Eq. (4), one obtains

$$\begin{aligned} A^{(I)}(s,t,u) = &\sum_{\ell=0}^{\ell_{\max}}(2\ell+1)P_\ell(z_s)p^{2\ell}(s)\bar{a}_\ell^{(I)}(s) \\ &+\sum_{\ell=0}^{\ell_{\max}}\sum_{I'}(2\ell+1)P_\ell(z_t)p^{2\ell}(t)\frac{1}{2}C_{II'}\bar{a}_\ell^{(I')}(t) \\ &+\sum_{\ell=0}^{\ell_{\max}}\sum_{I'}(2\ell+1)P_\ell(z_u)p^{2\ell}(u) \\ &\times\frac{1}{2}C_{II'}\bar{a}_\ell^{(I')}(u)(-1)^{I+I'}, \end{aligned} \tag{17}$$

where the coefficients $C_{II'}$ are the matrix elements of

$$C = \begin{bmatrix} \frac{2}{3} & 2 & \frac{10}{3} \\ \frac{2}{3} & 1 & -\frac{5}{3} \\ \frac{2}{3} & -1 & \frac{1}{3} \end{bmatrix}. \tag{18}$$

We again remind the reader that the functions $\bar{a}_\ell^{(I)}(s)$ have only a RHC, and for each of them we write a dispersion

relation with an arbitrary number of subtractions n,[2]

$$\bar{a}_\ell^{(I)}(s) = \sum_{j=0}^{n-1} \frac{\bar{a}_\ell^{(I)(j)}(s_1)}{j!}(s-s_1)^j + \frac{(s-s_1)^n}{\pi}\int_{s_{\rm th}}^{\infty} \mathrm{d}s' \frac{\mathrm{Im}\bar{a}_\ell^{(I)}(s')}{(s'-s_1)^n(s'-s)}, \tag{19}$$

where $s_{\rm th} = 4m^2$. For simplicity, all of the subtractions are taken at the same point $s_1 < s_{\rm th}$, and the subtraction constants are denoted as $\bar{a}_\ell^{(I)(j)}(s_1)$. As it is written, Eq. (19) might lead one to think that the subtraction constants have no physical meaning. This, however, depends on the subtraction point chosen and the contribution of the crossed channels. In any case, with appropriate (linear) transformations, the subtractions constants at any subthreshold point can be related to the effective range parameters [introduced in Eq. (11)]. We will see this in an specific case in Sect. 3. Dispersion relations similar to Eq. (19) are implied for the t- and u-channel isobars. Inserting this dispersive representation into Eq. (17), and the resulting amplitudes $A^{(I)}(s,t,u)$ into the partial-wave projection, Eq. (6), one obtains the KT representation of the partial-wave amplitudes of well-defined isospin in the s-channel,

$$(t_{\rm KT})_\ell^{(I)}(s) = p^{2\ell}(s)\bar{a}_\ell^{(I)}(s) + \sum_{\ell',I'}\sum_{j=0}^{n-1}(2\ell'+1)C_{II'}\frac{R_{\ell\ell'}^{(j)}(s)}{j!}\bar{a}_{\ell'}^{(I')(j)}(s_1) + \sum_{\ell',I'}(2\ell'+1)C_{II'}\frac{1}{\pi}\int_{s_{\rm th}}^{\infty}\mathrm{d}t' S_{\ell\ell'}^{(n)}(s,t')\frac{\mathrm{Im}\bar{a}_{\ell'}^{(I')}(t')}{(t'-s_1)^n}. \tag{20}$$

The following functions have been introduced above:

$$R_{\ell\ell'}^{(j)}(s) = \frac{1}{2}\int_{-1}^{+1}\mathrm{d}z\ (t(s,z)-s_1)^j\ P_\ell(z) \times P_{\ell'}(z_t(s,z))p^{2\ell'}(t(s,z)), \tag{21}$$

$$S_{\ell\ell'}^{(n)}(s,t') = \frac{1}{2}\int_{-1}^{+1}\mathrm{d}z \times \frac{(t(s,z)-s_1)^n\ P_\ell(z)P_{\ell'}(z_t(s,z))p^{2\ell'}(t(s,z))}{t'-t(s,z)}. \tag{22}$$

The functions $R_{\ell\ell'}^{(j)}(s)$ are polynomials in s. Furthermore, both $R_{\ell\ell'}^{(j)}(s)$ and $S_{\ell\ell'}^{(n)}(s,t')$ behave as $p^{2\ell}(s)$ for $s \to 4m^2$. In the s-channel physical region, Eq. (20), together with Eq. (19), can be written more compactly as a Roy-like equation,

$$(t_{\rm KT})_\ell^{(I)}(s) = p^{2\ell}(s) \times \left(P_\ell^{(I)}(s) + \sum_{\ell',I'}\int_{s_{\rm th}}^{\infty}\mathrm{d}t'\frac{Q_{\ell\ell'}^{II'}(s,t')}{p^{2\ell'}(t')}\mathrm{Im}(t_{\rm KT})_{\ell'}^{(I')}(t')\right), \tag{23}$$

where we used $\mathrm{Im}(t_{\rm KT})_\ell^{(I)}(s) = p^{2\ell}(s)\mathrm{Im}\bar{a}_\ell^{(I)}(s)$ for $s > s_{\rm th}$. The polynomial term[3] $P_\ell^{(I)}(s)$ and the integral kernels $Q_{\ell\ell'}^{II'}(s,t')$ are given by

$$P_\ell^{(I)}(s) = \sum_{\ell',I'}\sum_{j=0}^{n-1}\left(\frac{(s-s_1)^j}{j!}\bar{a}_{\ell'}^{(I')(j)}(s_1)\delta_{\ell\ell'}\delta^{II'} + (2\ell'+1)C_{II'}\frac{R_{\ell\ell'}^{(j)}(s)}{p^{2\ell}(s)}\frac{\bar{a}_{\ell'}^{(I')(j)}(s_1)}{j!}\right), \tag{24}$$

$$Q_{\ell\ell'}^{II'}(s,t') = \frac{1}{\pi(t'-s_1)^n}\left[\frac{(s-s_1)^n}{t'-s}\delta_{\ell\ell'}\delta^{II'} + C_{II'}(2\ell'+1)\frac{S_{\ell\ell'}^{(n)}(s,t')}{p^{2\ell}(s)}\right]. \tag{25}$$

This is our final form of the KT equations for $\pi\pi$ scattering.

3 Analytical comparison of KT and Roy equations for S- and P-waves

We begin in this section with a brief introduction to the Roy equations before comparing them with the KT equations developed in Sect. 2. The Roy equations have been used extensively to study $\pi\pi$ scattering, with initial studies following Roy's original paper [46–50], but also more recently in the context of newer data [39,40]. The Roy equations impose, within a given kinematical region, rigorous conditions on the determination of partial-wave amplitudes of definite isospin, based on analyticity and crossing symmetry. In their exact form, the Roy equations couple the infinite set of partial waves. However, any practical application requires a finite truncation, which makes them resemble the KT equations as we will demonstrate. The starting point for deriving these equations is to write down a twice-subtracted fixed-t dispersion relation for these amplitudes. Roy realized these could be written as a matrix equation [33]:

$$A^{(I)}(s,t,u) = \sum_{I'}(C_{st})_{II'}\left[\alpha_{I'}(t)+\beta_{I'}(t)(s-u)\right] + \frac{1}{\pi}\int_{s_{\rm th}}^{\infty}\frac{\mathrm{d}x}{x^2}\left(\frac{s^2}{x^2-s^2}\delta_{II'} + \frac{u^2}{x^2-u^2}(C_{us})_{II'}\right) \times \mathrm{Im}A^{(I')}(x,t,u(x,t)), \tag{26}$$

[2] Strictly speaking, it is more correct to write $n = n_{\ell,I}$ since the number of subtractions performed can vary for each wave. While this possibility has been explored, the results presented in Sect. 4 consider only the same number of subtractions for all waves.

[3] The explicit form of the polynomial contributions $P_\ell^{(I)}(s)$ is shown in Appendix B for the cases $n = 1$ and $n = 2$.

where we are using the notation in Eq. (4). The column vectors characterizing the t-dependent subtraction constants $\alpha_{I'}(t)$ and $\beta_{I'}(t)$ have isospin 0, 2 and isospin 1 components, respectively. The matrices $(C_{st})_{II'}$ and $(C_{su})_{II'}$ are the crossing matrices and are given explicitly in Ref. [33].[4] The Roy equations themselves are the partial-wave projection of Eq. (26). Using the notation of Ref. [39], these can be compactly written as

$$(t_{\rm Roy})_\ell^{(I)}(s) = k_\ell^{(I)}(s) + \sum_{\ell',I'} \int_{s_{\rm th}}^{\infty} {\rm d}x\, K_{\ell\ell'}^{II'}(s,x) \times {\rm Im}\,(t_{\rm Roy})_{\ell'}^{(I')}(x). \tag{27}$$

In this equation, the kinematical functions $k_\ell^{(I)}(s)$ are known linear polynomials in s resulting from projecting over the subtraction polynomials. They contain two parameters; the $S0$- and $S2$-wave scattering lengths $a_0^{(0)}$ and $a_0^{(2)}$, respectively. The integral kernels $K_{\ell\ell'}^{II'}(s,x)$ are known as well and are fully documented in Appendix A of Ref. [39]. Including the results of Refs. [51,52] with experimental information on the scattering lengths and imaginary parts ${\rm Im}\,(t_{\rm Roy})_{\ell'}^{(I')}(s)$ for $s_{\rm th} < s < \infty$, the real part of Eq. (27) can be fully determined on the interval $-4m^2 < s < 60m^2$, and analytically continued to the complex plane in a region limited by the Lehmann ellipse [39]. This implies the Roy equations are particularly useful for studying the resonance properties of low-energy $\pi\pi$ scattering. Indeed, they have proven to be a popular resource in this regard.

Now that we have introduced the Roy equations, we proceed by comparing them with our formalism of the KT equations. If restricted to the elastic region, the Roy equations Eq. (27) can be seen as a closed set of coupled nonlinear integral equations for amplitudes $(t_{\rm Roy})_\ell^{(I)}(s)$, since each of the former can be written in terms of a single function, the phase shift $\delta_\ell^{(I)}(s)$. The same can be said of the KT equations, but this approach will not be pursued here. We instead consider the Roy and KT equations as integral representations of the analytical partial waves in terms of their discontinuities and subtraction constants. As mentioned in Sect. 1, the aim in this section is to analytically compare the KT and Roy equations when truncating both formalisms to include only S- and P-waves ($\ell, \ell' = 0, 1$). One needs to consider the previous sentence with care: by truncation of the Roy equations to S- and P-waves, we mean letting the values of ℓ and ℓ' in Eq. (27) to be either 0 or 1. This truncation should not be confused with what is usually done in several analyses of the Roy equations [39,40,46–50], where one solves the integral equation for a finite number of low partial waves. Consequently, what we refer to as the Roy equations in comparison to the KT equations under truncation does not exactly coincide with those Roy equation analyses.

From Eq. (14), the KT amplitude $A(s,t,u)$ with $\ell_{\rm max} = 1$ has the expansion

$$A(s,t,u) = \frac{\bar a_0^{(0)}(s) - \bar a_0^{(2)}(s)}{3} + \frac{\bar a_0^{(2)}(t)}{2} + \frac{3}{8}(s-u)\bar a_1^{(1)}(t) + \frac{\bar a_0^{(2)}(u)}{2} + \frac{3}{8}(s-t)\bar a_1^{(1)}(u). \tag{28}$$

That the Roy equations imply this KT-like structure for $A(s,t,u)$, with the functions $\bar a_\ell^{(I)}(s)$ having only a RHC, has been already discussed in Refs. [34–39]. In what follows, we show in full detail that Roy and KT equations under the truncation specified give the same partial-wave amplitudes as in Eq. (28). To that end, let us consider a single subtraction $n = 1$ in each of the KT isobars. Since we are considering only one subtraction in each isobar, we simplify the notation throughout this section by writing $\bar a_\ell^{(I)(j=0)}(s_1) = \bar a_\ell^{(I)}(s_1)$. In this way, the KT polynomials of Eq. (24) are

$$P_0^{(0)}(s) = \frac{5}{3}\left(\bar a_0^{(0)}(s_1) + 2\bar a_0^{(2)}(s_1)\right) + \frac{3}{4}(3s - 4m^2)\bar a_1^{(1)}(s_1), \tag{29}$$

$$P_0^{(2)}(s) = \frac{2}{3}\left(\bar a_0^{(0)}(s_1) + 2\bar a_0^{(2)}(s_1)\right) - \frac{3}{8}(3s - 4m^2)\bar a_1^{(1)}(s_1), \tag{30}$$

$$P_1^{(1)}(s) = \frac{3}{2}\bar a_1^{(1)}(s_1). \tag{31}$$

Although we have made a total of three subtractions, there are only two effective parameters, the subtraction constant $\bar a_1^{(1)}(s_1)$ and the linear combination $\bar a_0^{(0)}(s_1) + 2\bar a_0^{(2)}(s_1)$. This is similar to what happens in the Roy equations. Let us now pay attention to the difference between the kernels of the KT and Roy equations,

$$\pi\,\Delta_{\ell\ell'}^{II'}(s,t') \equiv \frac{p^{2\ell}(s)}{p^{2\ell'}(t')} Q_{\ell\ell'}^{II'}(s,t') - K_{\ell\ell'}^{II'}(s,t'). \tag{32}$$

For instance, for the case $(\ell, I) = (0,0)$ and $(\ell', I') = (1,1)$ (recall that we are taking the number of subtractions $n = 1$), we have:

$$\frac{1}{p^2(t')} Q_{01}^{01}(s,t') = \frac{6}{\pi}\frac{2s + t' - 4m^2}{(t'-4m^2)(s-4m^2)} \log\left(1 + \frac{s-4m^2}{t'}\right) + 3\frac{4m^2 - 3s - 2(t'-s_1)}{\pi(t'-s_1)(t'-4m^2)}, \tag{33}$$

$$K_{01}^{01}(s,t') = \frac{6}{\pi}\frac{2s + t' - 4m^2}{(t'-4m^2)(s-4m^2)} \log\left(1 + \frac{s-4m^2}{t'}\right) + 3\frac{4m^2 - 3s - 2t'}{\pi t'(t'-4m^2)}. \tag{34}$$

It can be seen that the logarithmic terms cancel, and thus the difference is a first order polynomial in s. This happens for all $\Delta_{\ell\ell'}^{II'}(t',s)$ as long as $\ell, \ell' \leqslant 1$. Recalling that these

[4] They are related to the matrix C used in Sect. 2 through $(C_{st})_{II'} = \frac{1}{2}C_{II'}$ and $(C_{us})_{II'} = \frac{1}{2}C_{II'}(-1)^{I+I'}$.

differences appear under an integral in which the integration variable is t', we can write

$$
\begin{aligned}
(t_{\rm KT})_\ell^{(I)}(s) - (t_{\rm Roy})_\ell^{(I)}(s) &= p^{2\ell}(s) P_\ell^{(I)}(s) - k_\ell^{(I)}(s) \\
&+ \sum_{\ell', I'} \int_{s_{\rm th}}^{\infty} {\rm d}t' \Delta_{\ell\ell'}^{II'}(4m^2, t') \, {\rm Im}(t_{\rm Roy})_{\ell'}^{(I')}(t') \\
&+ (s - 4m^2) \sum_{\ell', I'} \int_{s_{\rm th}}^{\infty} {\rm d}t' \left[\frac{\partial}{\partial s} \Delta_{\ell\ell'}^{II'}(4m^2, t') \right] {\rm Im}(t_{\rm Roy})_{\ell'}^{(I')}(t') \\
&\equiv p^{2\ell}(s) P_\ell^{(I)}(s) - k_\ell^{(I)}(s) + x_\ell^{(I)} + (s - 4m^2) y_\ell^{(I)}, \qquad (35)
\end{aligned}
$$

where the imaginary part ${\rm Im}(t_{\rm KT})_{\ell'}^{(I')}(t') = {\rm Im}(t_{\rm Roy})_{\ell'}^{(I')}(t')$ are given as an input, and $x_\ell^{(I)}$ and $y_\ell^{(I)}$ are constants not depending on s. Moreover, they are related through:

$$
6y_1^{(1)} = -2y_0^{(2)} = y_0^{(0)} = \frac{2x_0^{(0)} - 5x_0^{(2)}}{12m^2}. \qquad (36)
$$

The above difference $(t_{\rm KT})_\ell^{(I)}(s) - (t_{\rm Roy})_\ell^{(I)}(s)$ is also a linear polynomial in s. The next question is: can we choose our constants $\bar{a}_1^{(1)}(s_1)$ and $\bar{a}_0^{(0)}(s_1) + 2\bar{a}_0^{(2)}(s_1)$ such that $(t_{\rm KT})_\ell^{(I)}(s) - (t_{\rm Roy})_\ell^{(I)}(s) = 0$ for the three S- and P-waves? The P-wave is proportional to $(s - 4m^2)$, so $x_1^{(1)} = 0$. We thus have to satisfy five conditions with only two parameters. It turns out that the solution

$$
3\left(\bar{a}_0^{(0)}(s_1) + 2\bar{a}_0^{(2)}(s_1)\right) = \left(a_0^{(0)} + 2a_0^{(2)}\right) - \left(x_0^{(0)} + 2x_0^{(2)}\right), \qquad (37)
$$

$$
27m^2 \bar{a}_1^{(1)}(s_1) = \left(2a_0^{(0)} - 5a_0^{(2)}\right) - \left(2x_0^{(0)} - 5x_0^{(2)}\right), \qquad (38)
$$

fulfills indeed the five conditions.[5] Hence, we have proved that, under the conditions indicated above,

$$
(t_{\rm KT})_\ell^{(I)}(s) - (t_{\rm Roy})_\ell^{(I)}(s) = 0. \qquad (39)
$$

This is a highly nontrivial result: the kernels of both approaches are originally different, but it turns out that they are such that the differences in the partial-wave amplitudes are only polynomials, and that the three polynomials can be put to zero with only two free parameters.

For higher waves, $\ell, \ell' \geqslant 2$, the kernels $K_{\ell\ell'}^{II'}(s, t')$ have more complicated structures. For instance, when $\ell' = 2$, one also finds the term $\log\left(1 + \frac{s-4m^2}{2t'}\right)$, in addition to $\log\left(1 + \frac{s-4m^2}{t'}\right)$. In that case, the differences in the kernels are not purely polynomials, and the above result cannot be proved.

[5] As advanced in Sect. 3, we explicitly see in Eqs. (37) and (38) that the subtraction constants can be linearly related to the threshold parameters.

4 Numerical results

Since the proof of the result in the previous section only holds when restricting to S- and P-waves, in this section we numerically study to what extent the KT equations are useful when higher partial waves are considered. Specifically, we now set $\ell_{\rm max} = 3$ in Eq. (14) and thus consider up to the F-wave. In this way, partial waves with $\ell \geqslant 4$ (G- and higher waves) are set to zero, and do not contribute to the imaginary parts in Eq. (23). As stated above, the KT and Roy equations give the real part of the amplitudes once the imaginary part is given, up to a polynomial contribution. As an input for the KT equations, we shall use the CFD parameterization of Ref. [40], which we now briefly discuss. This work parameterizes the inelasticities $\eta_\ell^{(I)}(s)$ and phase shifts $\delta_\ell^{(I)}(s)$ of the partial-wave amplitudes, Eq. (10). Two different parameterizations are given in Ref. [40], called UFD and CFD, which respectively stand for unconstrained and constrained fit to data. They do not differ on the form of the parameterization but in the values the parameters take. In the UFD parameterization only the data are fitted, while in the CFD dispersive constraints are imposed on the amplitudes. Among these, the most relevant ones are the Roy and GKPY equations, which are, respectively, twice- and once-subtracted dispersion relations for the $\pi\pi$ amplitude. Hence, the amplitudes computed with the CFD parameterization satisfy, within uncertainties, these dispersive equations. Both parameterizations of Ref. [40] provide the phase shifts and inelasticities along the RHC. These quantities can be used as inputs to the Roy or GKPY equations so that the amplitudes can be computed at any point on the complex plane. The real part of the amplitudes obtained with the Roy or GKPY equations along the RHC are very similar to those obtained with the CFD parameterization for the amplitudes, since the latter are constrained to satisfy the former. We can use as well the CFD parameterization of Ref. [40] as an input for our KT equations to obtain the real part of the partial-wave amplitudes $(t_{\rm KT})_\ell^{(I)}(s)$, and compare our results with the original input.

The real parts of the input amplitudes are the black solid lines in Fig. 1. The CFD parameterization reaches up to a center-of-mass energy squared $s_m = (1.42\ {\rm GeV})^2 \simeq 2\ {\rm GeV}^2$. Since the dispersive integrals in the KT equations extend to infinity, we shall take as an approximation $\delta_\ell^{(I)}(s) = \delta_\ell^{(I)}(s_m)$ and $\eta_\ell^{(I)}(s) = \eta_\ell^{(I)}(s_m)$ for $s \geqslant s_m$. It is important to mention here that we do not use the full CFD parameterization since above $s \simeq 2\ {\rm GeV}^2$ we set the phase shift to a constant instead of using the Regge formulas of Ref. [40]. With the input amplitudes fixed, the only remaining freedom in the KT equations are the subtraction constants appearing in the polynomial terms. The subtraction constants are chosen so as to minimize the difference in the region $s_{\rm th} \leqslant s \leqslant s_f$ between the real part of the input amplitudes and those computed with the KT equations. To

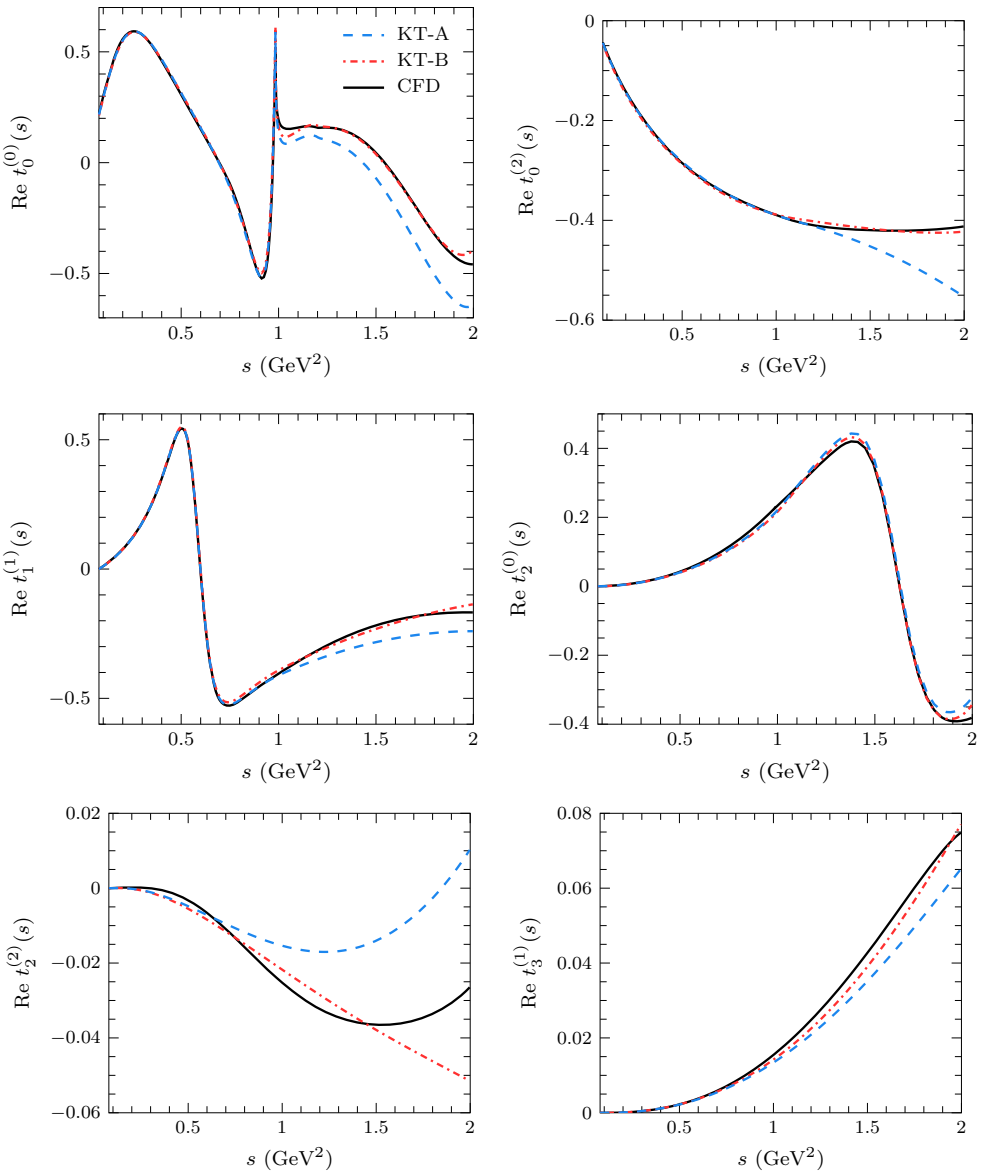

Fig. 1 Comparison of the real part of the different input partial-wave amplitudes $(t_{\rm CFD})_\ell^{(I)}(s)$ taken from Ref. [40] (black lines, labeled as CFD) with $(t_{\rm KT})_\ell^{(I)}(s)$. The two setups A (blue dashed line) and B (red dash-dotted line) represent different choices of the number of subtractions in each wave and the maximum value of s (s_f) taken into account into the fit of the subtraction constants (see text for more details)

be more specific, we are minimizing the following χ^2-like function:

$$\chi^2 = \frac{1}{s_f - s_{\rm th}} \sum_{\ell,I} \int_{s_{\rm th}}^{s_f} {\rm d}s \left({\rm Re}\left[(t_{\rm KT})_\ell^{(I)}(s) - (t_{\rm CFD})_\ell^{(I)}(s) \right] \right)^2 . \tag{40}$$

We recall that the goal here is not to describe the phase shifts and inelasticities parameterized in Ref. [40], but rather a comparison between the amplitudes used as an input and the output given by the KT equations. For this reason we will not dwell on the calculation of errors, which should be approximately equal to those given by the CFD parameterization. Two different setups for the fits will be considered. In setup A we choose for the number of subtractions $n = 1$ and $s_f = 1$ GeV^2, while setup B is computed with $n = 2$ and $s_f = 1.9$ GeV$^2 \lesssim s_m$,[6] where s_m has been defined

[6] In Setup B we choose $s_f = 1.9$ GeV^2 close to but smaller than $s_m \simeq 2$ GeV^2, in which our input for ${\rm Im}t_\ell^{(I)}(t')$ changes from the CFD parameterization to a constant phase and inelasticity one. By choosing $s_f \lesssim s_m$, we avoid the point $s = s_m$ in which, despite the fact that the amplitude is continuous, some small numerical perturbations could appear.

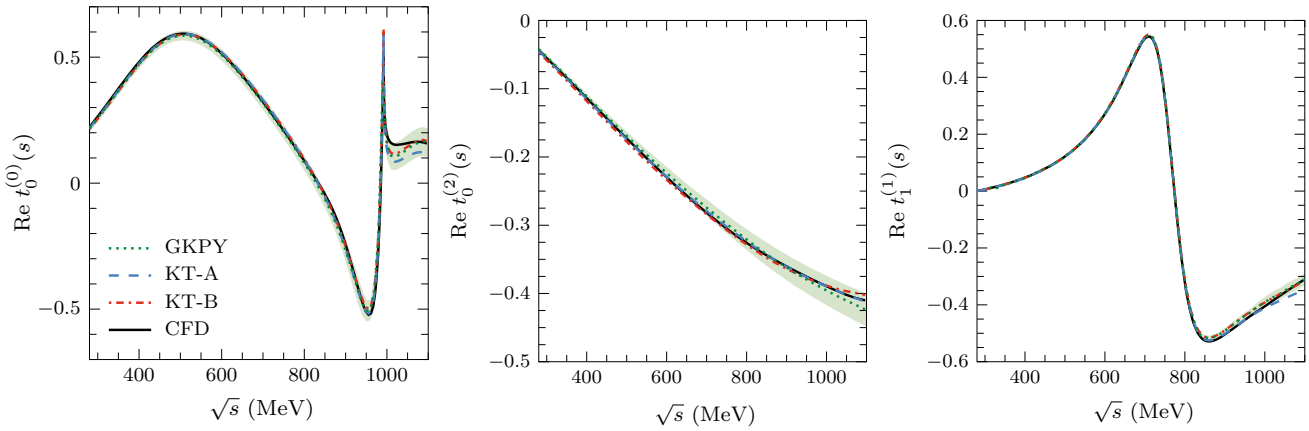

Fig. 2 Same as Fig. 1, but restricted to S- and P-waves, and including the dispersive output (green dotted lines, GKPY) of Ref. [40]. The (green) error band is associated with the GKPY dispersive output, as given in Ref. [40]

above. In setup A we seek a description of low energies with a small number of subtractions. In contrast, in setup B we have extended the range of the fit up to the maximum allowed by the CFD parameterization and the number of subtractions is increased.

In setup A, $n = 1$ and thus there are a total of six subtractions, but only five free parameters, since the subtraction constants $a_0^{(0)(0)}(s_1)$ and $a_0^{(2)(0)}(s_1)$ always appear in the same linear combination [see also the discussion in Sect. 3 and Eqs. (29)–(31)]. Analogously, in setup B, although $n = 2$ and there is a total of twelve subtractions, the number of free parameters is only seven and setup B introduces two additional free parameters with respect to setup A. The values of the χ^2-like function defined in Eq. (40) are $\chi^2 = 1.5 \cdot 10^{-3}$ and $2.7 \cdot 10^{-3}$ for setups A and B, respectively. We remark here that this is not a χ^2 function, and hence the comparison between the values for the two setups has no statistical meaning. We further remark that the inclusion of D- and F-waves is found to be necessary for an accurate description of the dispersive output with the KT equations, but only in the sense of the additional polynomial degrees of freedom they introduce. That is, the explicit inclusion of the imaginary contributions $\mathrm{Im}t_\ell^{(I)}(t')$ for $\ell > 1$ appearing in the dispersive projections in Eq. (23) are negligible. Despite the fact that these contributions are actually relevant over the entire interval $s \in (4m^2, \infty)$, their inclusion is typically smooth as we further discuss in the Appendix and their net contribution is found to be small in comparison to the aforementioned polynomials. The partial waves obtained within each setup are shown in Fig. 1. We see that the agreement with the original input is quite good and clearly better for setup B. In Fig. 2, showing only S- and P-waves up to $\sqrt{s} = 1.1$ GeV, we include in the comparison the dispersive output obtained with the GKPY equations and its associated error band, as given in Ref. [40]. We see that all curves lie well within or at the edges of the error bands.

Together with the general comparison of the real part of the input and KT amplitudes, we can more specifically compare the threshold parameters of the different waves that we have included in our study, cf. Eq. (11), obtained with the two approaches. In Table 1 we show the values of the $a_\ell^{(I)}$ and $b_\ell^{(I)}$ parameters computed with the KT equations and compared with those of Ref. [40] (the results labeled as CFD in that work are quoted here). We see that the agreement is also quite good. This is expected since these parameters control the low-energy behavior of the amplitudes, which the KT equations are able to reproduce in the whole energy range ($s_{\rm th} \leqslant s \leqslant s_m$) considered here.

Up to now we have checked the agreement between the real part of the amplitudes along the RHC obtained from KT equations and those from the CFD parameterization and the GKPY dispersive amplitudes of Ref. [40]. Since the subtraction constants have been fixed so as to minimize the difference between the input amplitudes and the output from the KT equations, this agreement could be seen as natural. One may therefore ask: to what extent does the agreement stand away from the real axis? In this context, the CFD parameterization of Ref. [40] is used in Refs. [53,54] to compute the amplitudes on the complex plane by means of GKPY and Roy equations, as described above. In particular, the position and coupling of poles associated with several resonances are computed in those works. As done with the Roy and GKPY equations, our KT equations allow us to compute the amplitudes at any point on the complex plane. Hence, we now compare the results obtained in Refs. [53,54] with those obtained with the KT equations. To that end, let us first briefly discuss the relation between resonances and amplitudes, mainly to define our notation. Resonances manifest in the amplitudes as poles on the unphysical Riemann sheets which are continuously connected with the physical one on the real axis. To reach the unphysical sheets the amplitudes must be ana-

Table 1 Threshold parameters and the pole positions and couplings for the σ, ρ, $f_0(980)$, and $f_2(1270)$ (the latter two are simply denoted above simply as f_0 and f_2, respectively) obtained with the KT equations (second and third columns for setups A and B, respectively) are shown. For comparison, we also show in the fourth column the same quantities extracted from the GKPY equations or the CFD parameterization of Ref. [40], as quoted in Refs. [40,53,54]

	KT-A	KT-B	GKPY–CFD	
$a_0^{(0)}$	0.217	0.213	0.221(9)	[40]
$b_0^{(0)}$	0.274	0.275	0.278(7)	[40]
$a_0^{(2)}$	−0.044	−0.047	−0.043(8)	[40]
$b_0^{(2)}$	−0.078	−0.079	−0.080(9)	[40]
$10^3 \cdot a_1^{(1)}$	37.5	37.9	38.5(1.2)	[40]
$10^3 \cdot b_1^{(1)}$	5.6	5.7	5.1(3)	[40]
$10^4 \cdot a_2^{(0)}$	17.8	17.8	18.8(4)	[40]
$10^4 \cdot b_2^{(0)}$	−3.4	−3.4	−4.2(1.0)	[40]
$10^4 \cdot a_2^{(2)}$	1.9	1.8	2.8(1.0)	[40]
$10^4 \cdot b_2^{(2)}$	−3.2	−3.2	−2.8(8)	[40]
$10^5 \cdot a_3^{(1)}$	5.7	5.7	5.1(1.3)	[40]
$10^5 \cdot b_3^{(1)}$	−4.0	−4.0	−4.6(2.5)	[40]
$\sqrt{s_\sigma}$ (MeV)	(448, 270)	(448, 269)	$(457^{+14}_{-13}, 279^{+11}_{-7})$	[53]
$\lvert g_\sigma \rvert$ GeV	3.36	3.37	$3.59^{+0.11}_{-0.13}$	[53]
$\sqrt{s_\rho}$ (MeV)	(762.2, 72.4)	(763.4, 73.5)	$(763.7^{+1.7}_{-1.5}, 73.2^{+1.0}_{-1.1})$	[53]
$\lvert g_\rho \rvert$	5.95	6.01	$6.01^{+0.04}_{-0.07}$	[53]
$\sqrt{s_{f_0}}$ (MeV)	(1000, 24)	(995, 26)	$(996 \pm 7, 25^{+10}_{-6})$	[53]
$\lvert g_{f_0} \rvert$ (GeV)	2.4	2.3	2.3 ± 0.2	[53]
$\sqrt{s_{f_2}}$ (MeV)	(1275.1, 89.5)	(1268.9, 86.4)	$(1267.3^{+0.8}_{-0.9}, 87 \pm 9)$	[54]
$\lvert g_{f_2} \rvert$ (GeV^{-1})	5.6	5.5	5.0 ± 0.3	[54]

lytically continued. Denoting as $t_{II}(s)$ the amplitude[7] on the second Riemann sheet, we take its customary definition in terms of the amplitude on the physical sheet, $t_I(s)$:

$$t_{II}^{-1}(s) = t_I^{-1}(s) + 2i\sigma(s). \tag{41}$$

Around the pole $s \simeq s_p$,

$$t_{II}(s) \simeq \frac{\tilde{g}_p^2}{s - s_p}, \tag{42}$$

and we define the coupling g_p of the resonance to the $\pi\pi$ channel in terms of the residue $\tilde{g}_p$ as[8]

$$g_p^2 = -16\pi \frac{2\ell + 1}{(4p^2(s_p))^\ell} \tilde{g}_p^2. \tag{43}$$

In Table 1 we show the poles and couplings of the different resonances that show up in the amplitudes considered in this work (S-, P-, D-, and F-waves). It can be seen that there is an excellent agreement between the determination obtained with the KT equations and those from the dispersive approach of Refs. [53,54], which use our same input amplitudes but into dispersive equations in principle very different from KT equations.

Our final discussion about the results for the partial-wave amplitudes obtained with the KT formalism concerns the unitarity of said amplitudes. As explained before, Ref. [40] parameterizes the amplitudes through the phase shifts $\delta_\ell^{(I)}(s)$ and inelasticities $\eta_\ell^{(I)}(s)$ as given in Eq. (10), with the latter chosen such that $\eta_\ell^{(I)}(s) \leqslant 1$. Hence, the input amplitudes are unitary by construction. However, there is nothing in the KT equations (neither in the Roy nor GKPY equations) that force the partial waves to fulfill unitarity. For instance, in the derivation of our KT equations in Sect. 2, the unitarity requirement is not used, and only dispersion relations for the different functions entering in the full amplitude $A(s, t, u)$ are used. A similar statement can be made about the Roy equations.[9] Unitarity is only achieved when a specific con-

[7] Here, for simplicity in the notation, we drop the ℓ, I scripts notation.

[8] We choose this particular definition of the coupling to directly compare with the results given in Refs. [40,53,54].

[9] As discussed for instance in Ref. [39], the unitarity of the partial wave is an additional requirement to be imposed on the Roy equations. The same can be said about the other dispersive approaches referred to in this

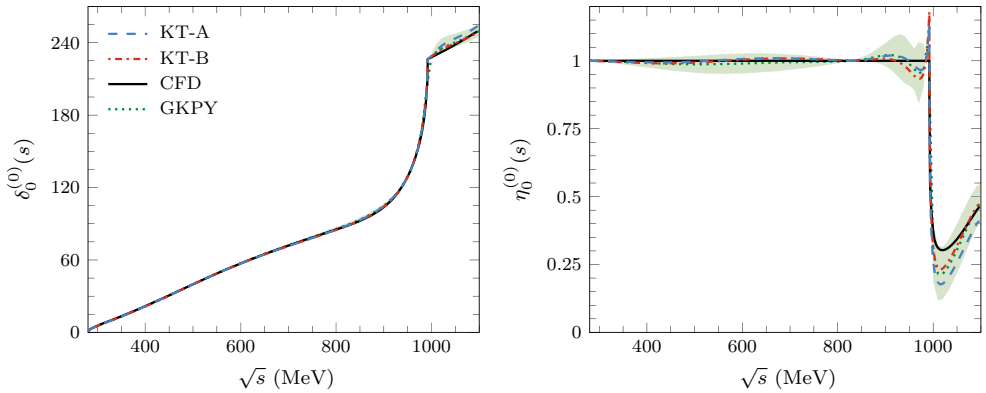

Fig. 3 Phase shift (left) and inelasticity (right) for the $S0$ wave. The notation for the different curves and the band is as in Fig. 2. These quantities are constructed from the real and imaginary parts of the $S0$ partial wave. The real part of the KT or GKPY amplitudes is given by the dispersive approach used (for instance, Eq. (20) for the KT approach), whereas the imaginary part, by construction, is given by the amplitude used to feed the dispersive equations. In both cases, this is the CFD parameterization

straint is imposed relating the real and the imaginary parts. A second point to be taken into account is that, as explained in Sect. 3, in this work we are not obtaining $t_\ell^{(I)}(s)$ as the solution of the *integral equation* in Eq. (23). Rather, our approach in this work is to consider Eq. (23) as an *integral representation* for the amplitude $t_\ell^{(I)}(s)$, which can be obtained when a given input (namely, a specific parameterization of the imaginary part) is used to *feed* the equations. The fact that the input used fulfills unitary does not guarantee that the amplitude obtained as an output will fulfill unitarity. Hence, in this approach, unitarity violations[10] are to be expected and, indeed, they are present. Yet, as we shall see below, we can advance the idea that using a unitary parameterization of the input amplitude makes these unavoidable unitary violations quite small.

Let us take as an example the S0 wave. In Fig. 3 we show the phase shift and inelasticity of this wave as given by the CFD parameterization of Ref. [40] (black solid line), and as obtained from $t_0^{(0)}(s)$ calculated with KT equations (blue dashed and red dash-dotted lines for setup A and B, respectively). Since the real part of $t_0^{(0)}(s)$ closely follows the input amplitude (see Figs. 1 and 2), and the imaginary parts are equal by construction, we expect $\delta_0^{(0)}(s)$ and $\eta_0^{(0)}(s)$ to be similar in both approaches and, indeed, they are. However, for $\sqrt{s} \leqslant 1$ GeV ($K\bar{K}$ threshold), we see that the input inelasticity is exactly one due to the parameterization. This is not the case for the KT equation, which shows a value $\eta_0^{(0)} \geqslant 1$ in a small region around $\sqrt{s} \simeq 1$ GeV. For low energies, $\eta_0^{(0)}$ is very close to 1, and for $\sqrt{s} \geqslant 1$ GeV the KT determination of $\eta_0^{(0)}$ closely follows the inelasticity of the input amplitude. We also show in Fig. 3 $\eta_0^{(0)}$ as computed with the partial wave that results from the GKPY equations (green dotted line), as well as a simple estimation of its error from one of the partial waves (see Fig. 2). We observe that our KT dispersive output lies well within this error band. Furthermore, the value $\eta_0^{(0)}(s) = 1$ for $s \leqslant 4m_K^2$ is well comprised in this error band. All this considered, and given that unitarity is not imposed in KT equations, we can safely say that unitarity is well fulfilled for low energies.

For higher energies, $s \to \infty$, due to the $p^{2\ell}(s)$ factors chosen in our definitions of the amplitudes to satisfy the threshold behavior, the absolute value of the real part of the partial-wave amplitudes grows as s^λ (with some positive integer λ), and then the inelasticity does not satisfy unitarity either. This behavior could be corrected by cutting the KT equation for $t_\ell^{(I)}(s)$ at some value of s and imposing there some appropriate asymptotic behavior, but this is beyond the scope of our exploratory study. Furthermore, as said, this unwanted behavior occurs for $s \to \infty$, whereas the KT equations are meant to be low-energy approximations.

5 Discussion and conclusions

In this work, we explored the various aspects of the KT formalism within the context of $\pi\pi$ scattering. Our main goal was to assess the validity of the KT formalism within a kinematical range characteristic of hadronic processes in general. Since $\pi\pi$ scattering is the most well studied and simplest, purely hadronic process, this makes it an ideal system for testing the KT formalism. To accomplish this, we derived the KT equations for $\pi\pi$ scattering in Sect. 2 and followed this with a proof showing the KT and Roy equations are equivalent when

Footnote 9 continued
paper. This can be achieved, for instance, by looking only for solutions in a subspace of unitary solutions.

[10] These refer to either $\eta_\ell^{(I)}(s) < 1$ in the elastic region, or $\eta_\ell^{(I)}(s) > 1$ in any region.

truncating both formalisms to include only S- and P-waves in Sect. 3. While the connection between the Roy equations and the reconstruction theorem under a similar truncation has already been made in previous works, here we demonstrated that a general representation of the amplitude in terms of three distinct expansions in all of the scattering channels also reproduces this result. Numerical results testing the validity of the KT equations including higher waves was explored in Sect. 4. The dispersive output from the KT equations using as an input the CFD parameterization of Ref. [40] up to the F-wave and a center-of-mass energy $\sqrt{s} = 1.42$ GeV was compared with the GKPY equations and the CFD input itself. The KT equations provide an excellent agreement with both the CFD parameterization and GKPY equations at the level of partial-wave amplitudes and subsequent resonance pole parameters. In addition, since the KT equations (as well as the Roy or GKPY equations) do not imply *per se* the unitarity of the partial waves, we have studied how much they deviate from exact unitarity. We found that the KT equations satisfy unitarity within the CFD parameterization error for low energies. This supports the idea that the KT formalism is a good and simple approach for modeling amplitudes at low energies. The contribution to the partial waves coming from the LHC in the KT approach is also explored in some detail. It is found that, in the scattering region, and for some waves, this contribution can be well accounted for by polynomials.

Acknowledgements MA and NS contributed equally to this work. MA thanks J. R. Peláez, A. Rodas, and J. Ruiz de Elvira for useful discussions and for providing numerical results concerning Ref. [40]. NS thanks E. Passemar for useful discussions. This work was supported by BMBF, by the U.S. Department of Energy under grants No. DE-AC05-06OR23177 and No. DE-FG02-87ER40365, by PAPIIT-DGAPA (UNAM, Mexico) grant No. IA101717, CONACYT (Mexico) grant No. 251817, by Research Foundation – Flanders (FWO), by U.S. National Science Foundation under award Nos. PHY-1415459 and PHY-1205019, and Ministerio de Economía y Competitividad through grants Nos. FPA2016-77313-P, FIS2014-51948-C2-1-P and SEV-2014-0398.

Funded by SCOAP[3].

Appendix A: LHC contributions

A dispersive representation of the $\pi\pi$ partial waves $t_\ell^{(I)}(s)$ would have, generally speaking, three different contributions: two terms from the integrals of the discontinuities along the RHC and LHC, and a polynomial term stemming from the subtractions performed in the dispersion relation. These contributions are easily identifiable in our KT representation of the partial waves, Eq. (23). The RHC and LHC respectively arise from the singular and nonsingular terms of the kernels, Eq. (25), whereas the polynomial term is given by Eq. (24). In this appendix we discuss the relative importance of the LHC contribution to the partial waves in the KT dispersive representation. In Fig. 4 we show, for the S- and P-waves, the three contributions to the partial waves, together with the total amplitude. For simplicity, we consider the number of subtractions given by setup A discussed above for the KT approach. We immediately mention two features. First, in the $S0$ and P waves, where prominent resonances show up, the general shape of the amplitude is given by that of the RHC contribution. Second, the LHC contribution is of non-negligible magnitude in the three waves. However, even if the LHC contribution is large, we see that, for the $S0$ and P waves, it has no particular structure in the region $s \leqslant 1$ GeV^2 (the maximum range for setup A), whereas it has a more complicated structure in the $S2$ wave. In Fig. 5 we show the LHC contribution for the three waves compared with order n polynomials, whose coefficients have been fitted to reproduce the LHC contribution. For the $S2$ wave, although the polynomial is able to account for the bulk of the LHC contribution, the particular details of the former cannot be described even with higher-order polynomials. Although

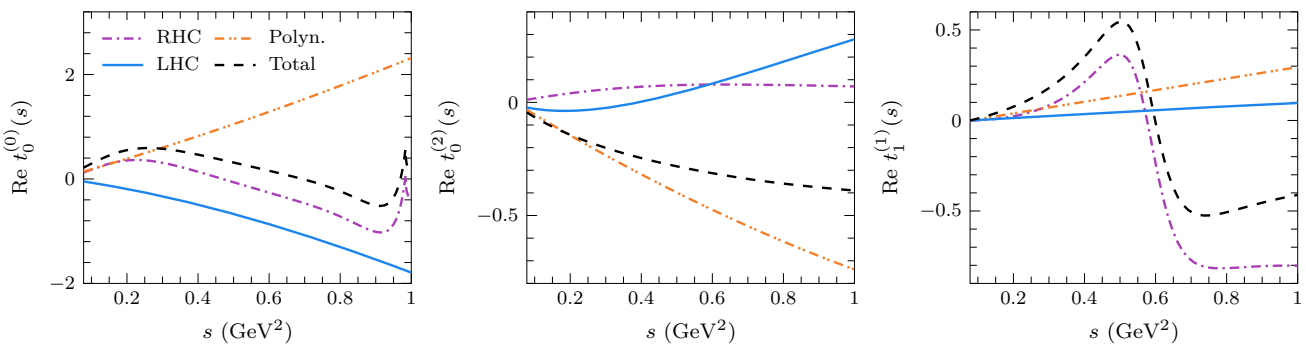

Fig. 4 Contributions to the total partial-wave amplitude using setup A as described above (black dashed line): RHC integral (purple dash-dotted line), LHC integral (blue solid line), and polynomial term (orange dash-double-dotted line). Only the S- and P-waves are shown

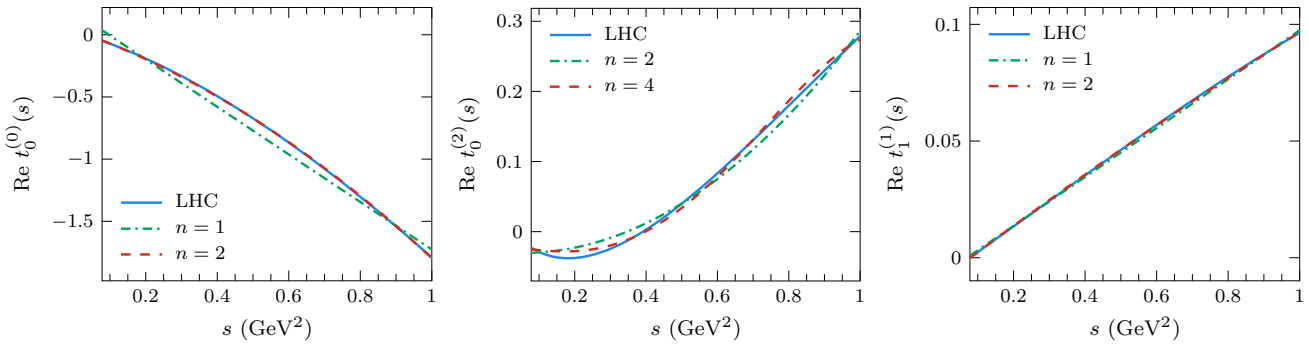

Fig. 5 Comparison of the LHC integral (blue solid line) shown in Fig. 4 with order n polynomials (red dashed and green dash-dotted lines) with coefficients fitted to reproduce the LHC integral

this agrees with the expectation for the LHC to dominate the $S2$ lineshape, in absence of any resonance pole, the deviations of the polynomial from the LHC are of the same order as the deviations of KT from the Roy result shown in Fig. 1, and we cannot derive any strong conclusions from that. On the other hand, for the $S0$ and P waves it can be seen that it is possible to accurately reproduce the LHC contribution with low-order polynomials. Therefore, if one writes down independent (i.e., crossing symmetry violating) dispersion relations for the partial waves $t_\ell^{(I)}(s)$, the contributions from the LHC can be reabsorbed into the polynomial coefficients that are already present in the dispersion relation for the RHC. This is the meaning of the common statement that LHC contributions can be neglected (or at least treated perturbatively) in scattering process like $\pi\pi \to \pi\pi$.

Appendix B: Polynomials

In this Appendix we collect the polynomials used in the KT equations, Eq. (24). The variable $\hat{s}$ stands for $\hat{s} = s/m^2$, and the analogous definition is implied for the subtraction point, $\hat{s}_1 = s_1/m^2$. For compactness, we have dropped the s_1 dependence in the subtraction constants, $\bar{a}_\ell^{(I)(j)}(s_1) \to \bar{a}_\ell^{(I)(j)}$. The first six equations, Eqs. (B1)–(B6), represent the polynomial contributions $P_\ell^{(I)}(s)$ (we remind the reader that the appropriate factors $p^{2\ell}(s)$ have been explicitly factored out) to the partial-wave amplitudes when one subtraction ($n = 1$, as in setup A) is performed on each isobar, $\bar{a}_\ell^{(I)}(s)$. Analogously, the six equations Eqs. (B7)–(B12) represent the additional contributions, $\Delta P_\ell^{(I)}(s)$, when two subtractions ($n = 2$, as in setup B) are performed.

$$
\begin{aligned}
P_0^{(0)}(s) &= \frac{5}{3}\bar{a}_0^{(0)(0)} + \frac{10}{3}\bar{a}_0^{(2)(0)} - 3\bar{a}_1^{(1)(0)} \\
&+ \frac{10}{9}\left(\bar{a}_2^{(0)(0)} + 5\bar{a}_2^{(2)(0)}\right) - \frac{7}{2}\bar{a}_3^{(1)(0)} \\
&+ \hat{s}\left(\frac{9}{4}\bar{a}_1^{(1)(0)} - \frac{20}{9}(\bar{a}_2^{(0)(0)} + 5\bar{a}_2^{(2)(0)}) + \frac{105}{8}\bar{a}_3^{(1)(0)}\right) \\
&+ \hat{s}^2\left(\frac{25}{36}(\bar{a}_2^{(0)(0)} + 5\bar{a}_2^{(2)(0)}) - \frac{315}{32}\bar{a}_3^{(1)(0)}\right) \\
&+ \frac{245}{128}\hat{s}^3\bar{a}_3^{(1)(0)},
\end{aligned}
\tag{B1}
$$

$$
\begin{aligned}
P_0^{(2)}(s) &= \frac{2}{3}\bar{a}_0^{(0)(0)} + \frac{4}{3}\bar{a}_0^{(2)(0)} + \frac{3}{2}\bar{a}_1^{(1)(0)} \\
&+ \frac{5}{9}\left(2\bar{a}_2^{(0)(0)} + \bar{a}_2^{(2)(0)}\right) + \frac{7}{4}\bar{a}_3^{(1)(0)} \\
&+ \hat{s}\left(-\frac{9}{8}\bar{a}_1^{(1)(0)} - \frac{10}{9}(2\bar{a}_2^{(0)(0)} + \bar{a}_2^{(2)(0)}) - \frac{105}{16}\bar{a}_3^{(1)(0)}\right) \\
&+ \hat{s}^2\left(\frac{25}{72}(2\bar{a}_2^{(0)(0)} + \bar{a}_2^{(2)(0)}) + \frac{315}{64}\bar{a}_3^{(1)(0)}\right) - \frac{245}{256}\hat{s}^3\bar{a}_3^{(1)(0)},
\end{aligned}
\tag{B2}
$$

$$
\begin{aligned}
P_1^{(1)}(s) &= \left(4320\bar{a}_1^{(1)(0)} - 800(2\bar{a}_2^{(0)(0)}\right. \\
&\left. - 5\bar{a}_2^{(2)(0)}) + 3024\bar{a}_3^{(1)(0)}\right)\frac{1}{2880} \\
&+ \left(1000(2\bar{a}_2^{(0)(0)} - 5\bar{a}_2^{(2)(0)}) - 9072\bar{a}_3^{(1)(0)}\right)\frac{\hat{s}}{2880} \\
&+ \frac{441}{320}\hat{s}^2\bar{a}_3^{(1)(0)},
\end{aligned}
\tag{B3}
$$

$$
P_2^{(0)}(s) = \frac{5}{9}(2\bar{a}_2^{(0)(0)} + \bar{a}_2^{(2)(0)}) - \frac{7}{10}\bar{a}_3^{(1)(0)} + \frac{49}{40}\hat{s}\,\bar{a}_3^{(1)(0)},
\tag{B4}
$$

$$
\begin{aligned}
P_2^{(2)}(s) &= -\frac{49}{80}\hat{s}\,\bar{a}_3^{(1)(0)} \\
&+ \frac{1}{720}\left(80\bar{a}_2^{(0)(0)} + 760\bar{a}_2^{(2)(0)} + 252\bar{a}_3^{(1)(0)}\right),
\end{aligned}
\tag{B5}
$$

$$
P_3^{(1)}(s) = \frac{21}{20}\bar{a}_3^{(1)(0)}.
\tag{B6}
$$

$$
\begin{aligned}
\Delta P_0^{(0)}(s) &= \frac{4}{3}\bar{a}_0^{(0)(1)} - \frac{5}{3}\hat{s}_1\bar{a}_0^{(0)(1)} + \frac{2}{9}\left(30\bar{a}_0^{(2)(1)} - 18\bar{a}_1^{(1)(1)}\right. \\
&\left. + 5(\bar{a}_2^{(0)(1)} + 5\bar{a}_2^{(2)(1)})\right) - \frac{14}{5}\bar{a}_3^{(1)(1)} \\
&- \frac{1}{9}\hat{s}_1\left(30\bar{a}_0^{(2)(1)} - 27\bar{a}_1^{(1)(1)}\right. \\
&\left. + 10(\bar{a}_2^{(0)(1)} + 5\bar{a}_2^{(2)(1)})\right) + \frac{7}{2}\hat{s}_1\bar{a}_3^{(1)(1)} \\
&+ \hat{s}\left(\frac{2}{3}\bar{a}_0^{(0)(1)} + \frac{1}{36}\left(-60\bar{a}_0^{(2)(1)} + 9(20 - 9\hat{s}_1)\bar{a}_1^{(1)(1)}\right.\right. \\
&\left.\left. + 10(-11 + 8\hat{s}_1)(\bar{a}_2^{(0)(1)} + 5\bar{a}_2^{(2)(1)})\right)\right.
\end{aligned}
$$

$$+\frac{133}{10}\bar{a}_3^{(1)(1)}-\frac{105}{8}\hat{s}_1\bar{a}_3^{(1)(1)}\Big)$$
$$+\hat{s}^2\left(\frac{1}{72}(-72\bar{a}_1^{(1)(1)}-25(-5+2\hat{s}_1)(\bar{a}_2^{(0)(1)}\right.$$
$$\left.+5\bar{a}_2^{(2)(1)}))-\frac{567}{40}\bar{a}_3^{(1)(1)}+\frac{315}{32}\hat{s}_1\bar{a}_3^{(1)(1)}\right)$$
$$+\hat{s}^3\left(-\frac{25}{96}(\bar{a}_2^{(0)(1)}+5\bar{a}_2^{(2)(1)})\right.$$
$$\left.+\frac{833}{160}\bar{a}_3^{(1)(1)}-\frac{245}{128}\hat{s}_1\bar{a}_3^{(1)(1)}\right)-\frac{49}{80}\hat{s}^4\bar{a}_3^{(1)(1)}, \tag{B7}$$

$$\Delta P_0^{(2)}(s)=\frac{4}{3}\bar{a}_0^{(0)(1)}-\frac{2}{3}\hat{s}_1\bar{a}_0^{(0)(1)}+\frac{2}{3}\bar{a}_0^{(2)(1)}$$
$$-\frac{4}{3}\hat{s}_1\bar{a}_0^{(2)(1)}+2\bar{a}_1^{(1)(1)}-\frac{3}{2}\hat{s}_1\bar{a}_1^{(1)(1)}$$
$$-\frac{5}{9}(-1+\hat{s}_1)(2\bar{a}_2^{(0)(1)}+\bar{a}_2^{(2)(1)})$$
$$+\frac{7}{5}\bar{a}_3^{(1)(1)}+\frac{49}{160}\hat{s}^4\bar{a}_3^{(1)(1)}-\frac{7}{4}\hat{s}_1\bar{a}_3^{(1)(1)}$$
$$+\hat{s}\left(-\frac{1}{3}\bar{a}_0^{(0)(1)}+\frac{5}{6}\bar{a}_0^{(2)(1)}-\frac{5}{2}\bar{a}_1^{(1)(1)}\right.$$
$$+\frac{9}{8}\hat{s}_1\bar{a}_1^{(1)(1)}-\frac{55}{36}(2\bar{a}_2^{(0)(1)}+\bar{a}_2^{(2)(1)})$$
$$\left.+\frac{10}{9}\hat{s}_1(2\bar{a}_2^{(0)(1)}+\bar{a}_2^{(2)(1)})-\frac{133}{20}\bar{a}_3^{(1)(1)}+\frac{105}{16}\hat{s}_1\bar{a}_3^{(1)(1)}\right)$$
$$+\hat{s}^2\left(\frac{1}{2}\bar{a}_1^{(1)(1)}+\frac{125}{144}(2\bar{a}_2^{(0)(1)}+\bar{a}_2^{(2)(1)})\right.$$
$$\left.-\frac{25}{72}\hat{s}_1(2\bar{a}_2^{(0)(1)}+\bar{a}_2^{(2)(1)})+\frac{567}{80}\bar{a}_3^{(1)(1)}-\frac{315}{64}\hat{s}_1\bar{a}_3^{(1)(1)}\right)$$
$$+\hat{s}^3\left(-\frac{25}{192}(2\bar{a}_2^{(0)(1)}+\bar{a}_2^{(2)(1)})-\frac{833}{320}\bar{a}_3^{(1)(1)}\right.$$
$$\left.+\frac{245}{256}\hat{s}_1\bar{a}_3^{(1)(1)}\right), \tag{B8}$$

$$\Delta P_1^{(1)}(s)=\frac{4}{9}\bar{a}_0^{(0)(1)}-\frac{10}{9}\bar{a}_0^{(2)(1)}-\frac{3}{2}\hat{s}_1\bar{a}_1^{(1)(1)}$$
$$+\frac{1}{9}(-2+5\hat{s}_1)\bar{a}_2^{(0)(1)}$$
$$-\frac{5}{18}(-2+5\hat{s}_1)\bar{a}_2^{(2)(1)}-\frac{7}{60}(-4+9\hat{s}_1)\bar{a}_3^{(1)(1)}$$
$$+\hat{s}\left(\frac{3}{2}\bar{a}_1^{(1)(1)}+\frac{1}{9}\bar{a}_2^{(0)(1)}-\frac{25}{36}\hat{s}_1\bar{a}_2^{(0)(1)}\right.$$
$$\left.-\frac{5}{18}\bar{a}_2^{(2)(1)}+\frac{125}{72}\hat{s}_1\bar{a}_2^{(2)(1)}+\frac{7}{20}(-4+9\hat{s}_1)\bar{a}_3^{(1)(1)}\right)$$
$$+\hat{s}^2\left(\frac{1}{8}\bar{a}_2^{(0)(1)}-\frac{5}{16}\bar{a}_2^{(2)(1)}-\frac{49}{320}(-4+9\hat{s}_1)\bar{a}_3^{(1)(1)}\right), \tag{B9}$$

$$\Delta P_2^{(0)}(s)=\frac{1}{360}\left(288\bar{a}_1^{(1)(1)}-80\bar{a}_2^{(0)(1)}-400\hat{s}_1\bar{a}_2^{(0)(1)}\right.$$
$$\left.-400\bar{a}_2^{(2)(1)}-200\hat{s}_1\bar{a}_2^{(2)(1)}+36(4+7\hat{s}_1)\bar{a}_3^{(1)(1)}\right)$$
$$+\frac{1}{360}\hat{s}\left(540\bar{a}_2^{(0)(1)}+900\bar{a}_2^{(2)(1)}-828\bar{a}_3^{(1)(1)}\right.$$
$$\left.-441\hat{s}_1\bar{a}_3^{(1)(1)}\right)+\frac{8}{5}\hat{s}^2\bar{a}_3^{(1)(1)}, \tag{B10}$$

$$\Delta P_2^{(2)}(s)=\frac{1}{720}\left(-288\bar{a}_1^{(1)(1)}-160\bar{a}_2^{(0)(1)}-80\hat{s}_1\bar{a}_2^{(0)(1)}\right.$$
$$\left.-80\bar{a}_2^{(2)(1)}-760\hat{s}_1\bar{a}_2^{(2)(1)}-36(4+7\hat{s}_1)\bar{a}_3^{(1)(1)}\right)$$
$$+\frac{1}{720}\hat{s}\left(360\bar{a}_2^{(0)(1)}+900\bar{a}_2^{(2)(1)}\right.$$
$$\left.+828\bar{a}_3^{(1)(1)}+441\hat{s}_1\bar{a}_3^{(1)(1)}\right)-\frac{4}{5}\hat{s}^2\bar{a}_3^{(1)(1)}, \tag{B11}$$

$$\Delta P_3^{(1)}(s)=\frac{2}{21}\bar{a}_2^{(0)(1)}-\frac{5}{21}\bar{a}_2^{(2)(1)}-\frac{1}{5}\bar{a}_3^{(1)(1)}$$
$$-\frac{21}{20}\hat{s}_1\bar{a}_3^{(1)(1)}+\frac{3}{2}\hat{s}\,\bar{a}_3^{(1)(1)}. \tag{B12}$$

References

1. A. Esposito, A. Pilloni, A.D. Polosa, Phys. Rep. **668**, 1 (2016). arXiv:1611.07920 [hep-ph]
2. R.F. Lebed, R.E. Mitchell, E.S. Swanson, Prog. Part. Nucl. Phys. **93**, 143 (2017). arXiv:1610.04528 [hep-ph]
3. S.L. Olsen, T. Skwarnicki, D. Zieminska, Rev. Mod. Phys. **90**, 015003 (2018). arXiv:1708.04012 [hep-ph]
4. M.T. Hansen, S.R. Sharpe, Phys. Rev. D **92**, 114509 (2015). arXiv:1504.04248 [hep-lat]
5. H.W. Hammer, J.Y. Pang, A. Rusetsky, JHEP **10**, 115 (2017). arXiv:1707.02176 [hep-lat]
6. R.A. Briceño, M.T. Hansen, S.R. Sharpe, Phys. Rev. D **95**, 074510 (2017). arXiv:1701.07465 [hep-lat]
7. I. Caprini, G. Colangelo, H. Leutwyler, Phys. Rev. Lett. **96**, 132001 (2006). arXiv:hep-ph/0512364 [hep-ph]
8. M. Albaladejo, J.A. Oller, Phys. Rev. D **86**, 034003 (2012). arXiv:1205.6606 [hep-ph]
9. J.R. Peláez, Phys. Rep. **658**, 1 (2016). arXiv:1510.00653 [hep-ph]
10. N.N. Khuri, S.B. Treiman, Phys. Rev. **119**, 1115 (1960)
11. J.B. Bronzan, C. Kacser, Phys. Rev. **132**, 2703 (1963)
12. I.J.R. Aitchison, Phys. Rev. **137**, B1070 (1965)
13. I.J.R. Aitchison, R. Pasquier, Phys. Rev. **152**, 1274 (1966)
14. R. Pasquier, J.Y. Pasquier, Phys. Rev. **170**, 1294 (1968)
15. R. Pasquier, J.Y. Pasquier, Phys. Rev. **177**, 2482 (1969)
16. A. Neveu, J. Scherk, Ann. Phys. **57**, 39 (1970)
17. I.J.R. Aitchison, Unitarity, analyticity and crossing symmetry in two- and three-hadron final state interactions (2015). arXiv:1507.02697 [hep-ph]
18. J. Stern, H. Sazdjian, N.H. Fuchs, Phys. Rev. D **47**, 3814 (1993). arXiv:hep-ph/9301244 [hep-ph]
19. M. Zdrahal, J. Novotny, Phys. Rev. D **78**, 116016 (2008). arXiv:0806.4529 [hep-ph]
20. J. Bijnens, K. Ghorbani, JHEP **11**, 030 (2007). arXiv:0709.0230 [hep-ph]
21. J. Kambor, C. Wiesendanger, D. Wyler, Nucl. Phys. B **465**, 215 (1996). arXiv:hep-ph/9509374 [hep-ph]
22. A.V. Anisovich, H. Leutwyler, Phys. Lett. B **375**, 335 (1996). arXiv:hep-ph/9601237 [hep-ph]
23. P. Guo, I.V. Danilkin, D. Schott, C. Fernández-Ramírez, V. Mathieu, A.P. Szczepaniak, Phys. Rev. D **92**, 054016 (2015). arXiv:1505.01715 [hep-ph]
24. P. Guo, I.V. Danilkin, C. Fernández-Ramírez, V. Mathieu, A.P. Szczepaniak, Phys. Lett. B **771**, 497 (2017). arXiv:1608.01447 [hep-ph]
25. G. Colangelo, S. Lanz, H. Leutwyler, E. Passemar, Phys. Rev. Lett. **118**, 022001 (2017). arXiv:1610.03494 [hep-ph]
26. M. Albaladejo, B. Moussallam, Eur. Phys. J. C **77**, 508 (2017). arXiv:1702.04931 [hep-ph]
27. F. Niecknig, B. Kubis, S.P. Schneider, Eur. Phys. J. C **72**, 2014 (2012). arXiv:1203.2501 [hep-ph]

28. I.V. Danilkin, C. Fernández-Ramírez, P. Guo, V. Mathieu, D. Schott, M. Shi, A.P. Szczepaniak, Phys. Rev. D **91**, 094029 (2015). arXiv:1409.7708 [hep-ph]
29. T. Isken, B. Kubis, S.P. Schneider, P. Stoffer, Eur. Phys. J. C **77**, 489 (2017). arXiv:1705.04339 [hep-ph]
30. F. Niecknig, B. Kubis, JHEP **10**, 142 (2015). arXiv:1509.03188 [hep-ph]
31. A. Pilloni, C. Fernández-Ramírez, A. Jackura, V. Mathieu, M. Mikhasenko, J. Nys, A.P. Szczepaniak, (JPAC), Phys. Lett. B **772**, 200 (2017). arXiv:1612.06490 [hep-ph]
32. F. Niecknig, B. Kubis, Phys. Lett. B **780**, 471 (2018). arXiv:1708.00446 [hep-ph]
33. S.M. Roy, Phys. Lett. **36B**, 353 (1971)
34. G. Mahoux, S.M. Roy, G. Wanders, Nucl. Phys. B **70**, 297 (1974)
35. M. Knecht, B. Moussallam, J. Stern, N.H. Fuchs, Nucl. Phys. B **457**, 513 (1995). arXiv:hep-ph/9507319 [hep-ph]
36. M. Knecht, B. Moussallam, J. Stern, N.H. Fuchs, Nucl. Phys. B **471**, 445 (1996). arXiv:hep-ph/9512404 [hep-ph]
37. B. Ananthanarayan, D. Toublan, G. Wanders, Phys. Rev. D **51**, 1093 (1995). arXiv:hep-ph/9410302 [hep-ph]
38. B. Ananthanarayan, Phys. Rev. D **58**, 036002 (1998). arXiv:hep-ph/9802338 [hep-ph]
39. B. Ananthanarayan, G. Colangelo, J. Gasser, H. Leutwyler, Phys. Rep. **353**, 207 (2001). arXiv:hep-ph/0005297 [hep-ph]
40. R. García-Martín, R. Kamiński, J.R. Peláez, J. Ruiz de Elvira, F.J. Ynduráin, Phys. Rev. D **83**, 074004 (2011). arXiv:1102.2183 [hep-ph]
41. V. Meshcheryakov, D. Shirkov, V. Serebryakov, *Dispersion Theories of Strong Interactions at Low Energy* (North-Holland Publishing Company, Amsterdam, 1969)
42. S. Lanz, Determination of the quark mass ratio Q from $\eta \to 3\pi$. Ph.D. thesis, Bern University (2011)
43. A.P. Szczepaniak, Phys. Lett. B **757**, 61 (2016). arXiv:1510.01789 [hep-ph]
44. M. Albaladejo, J.A. Oller, Phys. Rev. C **84**, 054009 (2011). arXiv:1107.3035 [nucl-th]
45. M. Albaladejo, J.A. Oller, Phys. Rev. C **86**, 034005 (2012). arXiv:1201.0443 [nucl-th]
46. J.L. Basdevant, J.C. Le Guillou, H. Navelet, Nuovo Cim. A **7**, 363 (1972)
47. J.L. Basdevant, C.D. Froggatt, J.L. Petersen, Nucl. Phys. B **72**, 413 (1974)
48. J.L. Basdevant, C.D. Froggatt, J.L. Petersen, Phys. Lett. **41B**, 173 (1972)
49. J.L. Basdevant, C.D. Froggatt, J.L. Petersen, Phys. Lett. **41B**, 178 (1972)
50. M.R. Pennington, S.D. Protopopescu, Phys. Rev. D **7**, 1429 (1973)
51. A. Martin, Nuovo Cim. A **42**, 930 (1965)
52. A. Martin, Nuovo Cim. A **42**, 1219 (1966)
53. R. García-Martín, R. Kaminski, J.R. Peláez, J. Ruiz de Elvira, Phys. Rev. Lett. **107**, 072001 (2011). arXiv:1107.1635 [hep-ph]
54. J.A. Carrasco, J. Nebreda, J.R. Peláez, A.P. Szczepaniak, Phys. Lett. B **749**, 399 (2015). arXiv:1504.03248 [hep-ph]